AN IMPROVED METHODOLOGY FOR PREDICTING RANDOM SPECTRUM LOAD INTERACTION EFFECTS ON FATIGUE CRACK GROWTH

J. B. Chang,* R. M. Engle,** and M. Szamossi*

*Rockwell International, North American Aircraft Division, Los Angeles, California, U.S.A.
**U. S. Air Force Wright Aeronautical Laboratories, Flight Dynamics Laboratory, Wright-Patterson Air Force Base, Ohio, U.S.A.

ABSTRACT

Fatigue crack-growth data for center-through cracks contained in 2219-T851 aluminum plates subjected to random spectrum loadings were generated. A crack-growth prediction methodology which accounts for overload retardation and compressive load acceleration effects on fatigue crack-growth was developed using the generalized Willenborg retardation model as the base. Fatigue crack-growth analyses were performed employing the proposed methodology. Analytical predictions were correlated to the test data. Good correlations were shown.

KEY WORDS

Fatigue crack-growth; random spectrum loading; retardation; acceleration; 2219-T851 aluminum; fracture control plan.

INTRODUCTION

The implementation of fracture control plans on structures such as airframes requires the capability for accurate predictions of the fatigue crack-growth behavior under random spectrum loadings. In reality, all service flight loadings should be classified as the random cycle-by-cycle type of spectrum. Various cyclic load interactions take place in such a spectrum, which affects the growth behavior of a crack. Significant facts observed by investigators are (1) tensile overloads introduce retardation to the crack-growth of the cycles following the overloads, (2) compressive loads in compression-tension load cycles accelerate the crack growth, and (3) compressive loads in the tension-compression load cycles reduce the retardation effects introduced by the tensile overloads.

Many cyclic load interaction models have been proposed in the past. These include the Wheeler model (Wheeler, 1972); Willenborg model (Willenborg, 1971) and its modified version, the generalized Willenborg model, (Gallagher, 1974); Elber's closure model (Elber, 1971) and modified versions, including the generalized closure model proposed by Bell and Wolfman (1976) and the contact stress model formulated by Dill and Saff (1976); and the Vroman/Chang model (Chang, 1979a). However, none of the existing models are able to account for all of the aforementioned load interaction effects on crack-growth. A few of them have been shown to provide fairly good

predictions for crack growth under certain types of variable amplitude loadings. These include the generalized closure model and the contact stress model. Yet, to employ such models in performing crack-growth analyses on a production basis, either extensive crack-growth test data will be generated in order to obtain numerous empirical constants needed for the model, or lengthy computations will be performed. In any regard, high cost is inevitable. The need to develop a crack-growth methodology which is able to account for all those important load interaction effects, yet remain cost effective, is obvious.

A combined experimental and analytical program is currently being undertaken by Rockwell International for the U. S. Air Force. One of the primary objectives of this program is to develop an improved methodology which provides capabilities needed for accurate crack-growth-behavior predictions. The development work has been carried out in the first two phases of this three-phase research program. This paper presents the experimental and analytical results.

EXPERIMENTAL PROGRAM

A random cycle-by-cycle spectrum loading test program consisted of 13 tests; all test flight spectra simulating laod histories for either a multimission fighter or an advanced transport have been conducted. The test flight spectra were generated in terms of peaks and valleys using the computer program, SPECGN 1 (Dill, 1977), developed for random stress process simulations. For fighter spectra, cycle-by-cycle random stress histories based on the baseline load spectra for a typical fighter were generated for the air-to-air (A-A), air-to-ground (A-G), instrumentation and navigation (I&N), and composite missions. The generated peaks and valleys were in the form of percentage of design limit stress as shown in Fig. 1, 2, and 3.

For transport spectra, a typical transport aircraft use was defined by three mission profiles: assault, logistics, and training. Each mission was composed of four mission segments, including climb, cruise, gust, and descentLike the fighter case, ground loads were inserted at the beginning and end of each mission. Peaks and valleys for each mission segment were generated using SPECGN 1 in the form of stresses as shown in Table 1.

Test specimens used in this experimental program were of the ASTM standard center-cracked-tension (CCT) specimens machined from 2219-T851 aluminum plate. The center notches were installed by employing the electrical discharge machining (EDM) process, with the maximum width of the notch being less than 0.0254 cm.

All tests were conducted employing an MTS fatigue testing system. Applied loads were controlled by the Datum 70 servosystem, a computer-controlled fatigue test system. The Datum 70 servosystem acted as a waveform generator which provided command signal outputs to the MTS servocontroller. A schematic of the interrelationship of the MTS and Datum 70 servosystem is shown in Fig. 4. The EDM crack starter slot in each specimen was precracked to produce a total crack length (2c) of 0.762 cm, approximately. Precracking was done under constant amplitude cycling at a stress ratio R = 0, with maximum a cyclic stress of 68.95 MPa. All tests were run in ambient laboratory air at room temperature. The cyclic rate of each test was between 4 and 6 Hz, depending on factors such as load levels, load ranges, and the presence of compression loads. Crack growth was measured by a visual optics reading from precision scales attached to each side of the specimen adjacent to the EDM slot. Measurements were made and recorded after approximately each 0.127 cm increment of growth. The long edges of the specimens were restrained against lateral motion when subjected to compression loads.

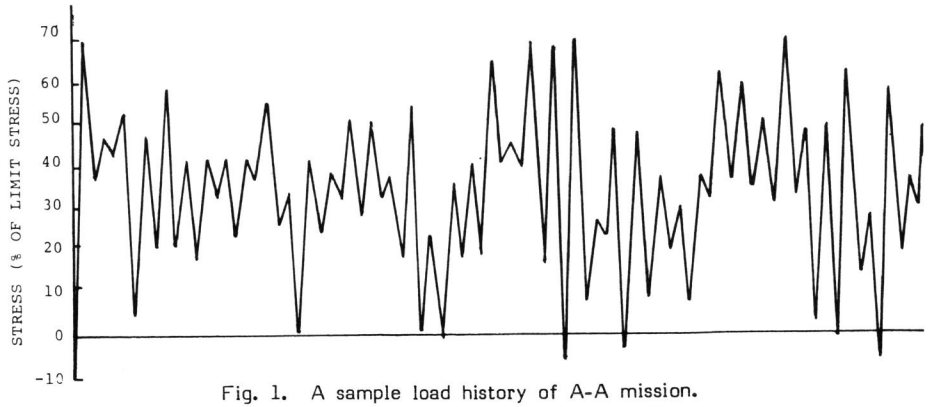

Fig. 1. A sample load history of A-A mission.

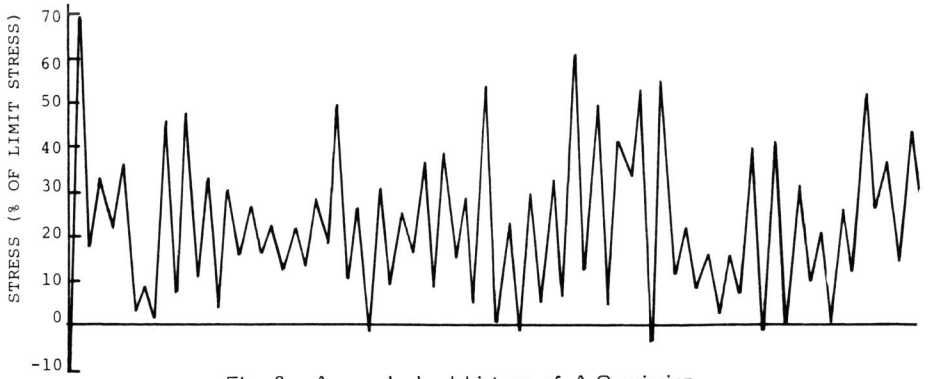

Fig. 2. A sample load history of A-G mission.

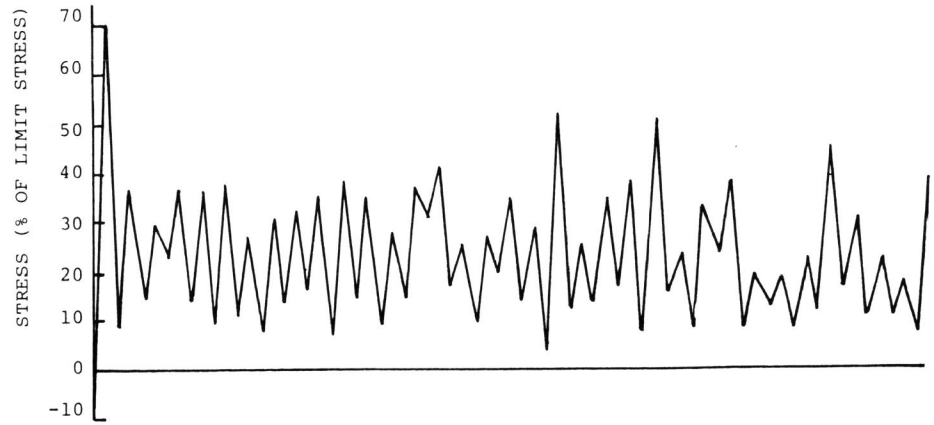

Fig. 3. A sample load history of I&N mission.

Table 1. A Portion of the Random Spectrum for a Typical Transport

Test M-93: This table as shown
M-94: 1.4 factor on this table

Line	Stresses in ksi*									
001	0.0	-6.4	10.8	10.7	10.9	10.8	10.8	10.3	12.5	8.4
	12.7	9.8	11.3	10.3	11.1	10.7	10.8	10.7	10.8	10.8
	10.8	10.7	11.2	9.3	12.2	10.2	10.9	10.5	11.4	10.5
	11.5	9.6	11.5	10.3	11.5	9.9	11.2	10.7	11.0	10.0
	11.4	10.7	10.7	10.7	11.1	10.7	10.8	10.7	10.8	10.7
	10.9	10.7	10.9	10.4	11.3	10.5	10.9	10.5	11.3	10.4
	11.0	10.1	12.5	8.6	12.3	10.1	11.0	10.8	10.8	10.6
	11.0	10.7	10.8	10.8	11.0	10.5	11.1	10.6	10.8	10.7
	11.3	10.0	11.2	10.6	11.3	9.8	11.7	9.9	11.9	10.1
010	10.8	10.8	11.0	10.2	11.5	10.3	11.1	10.8	10.8	10.8
	10.8	10.8	10.8	10.4	12.2	9.2	11.6	10.7	10.8	10.7
	11.0	10.6	11.0	10.7	10.8	10.8	10.9	10.7	10.8	10.7
	11.4	9.2	12.2	10.3	10.9	10.6	11.1	10.4	11.5	9.1
	9.8	9.0	9.1	9.0	9.2	9.1	9.1	8.7	10.7	6.8
	10.8	8.2	9.6	8.7	9.4	9.0	9.1	9.0	9.1	9.0
	9.1	9.0	9.4	7.7	10.4	8.5	9.2	8.9	9.6	8.8
	9.5	9.0	9.0	9.0	9.0	9.0	9.0	8.8	10.2	7.2
	10.4	8.4	9.3	8.7	9.2	8.9	9.0	9.0	9.0	9.0
	9.0	9.0	9.2	8.0	10.0	8.6	9.0	8.9	9.4	8.9
020	9.4	8.2	9.4	8.8	9.4	8.4	9.2	9.0	9.1	8.5
	9.4	9.0	9.0	9.0	9.1	9.0	9.0	9.0	9.0	9.0
	11.4	10.6	10.6	10.5	10.7	10.6	10.6	10.2	12.3	8.3
	12.5	9.7	11.2	10.2	10.9	10.5	10.7	10.6	10.7	10.6
	10.6	10.6	11.0	9.2	12.0	10.0	10.7	10.4	11.2	10.4
	11.3	9.5	11.3	10.2	11.3	9.7	11.0	10.6	10.8	9.8
	11.2	10.5	10.6	10.6	10.9	10.5	10.7	10.6	10.6	10.6
	10.7	10.6	10.7	10.3	11.1	10.4	10.7	10.4	11.1	10.2
	10.9	9.9	12.3	8.5	12.1	10.0	10.8	10.6	10.6	10.5
030	10.9	10.6	10.6	10.6	10.9	10.3	10.9	10.5	10.6	10.5
	11.1	9.8	11.0	10.4	11.1	9.7	11.5	9.8	11.7	-6.4
	12.9	9.1	11.5	10.6	10.8	10.7	10.8	10.8	10.8	10.7
	11.2	9.6	12.4	9.6	11.2	10.6	11.1	10.4	10.9	10.2
	11.2	10.7	10.8	10.7	11.3	10.1	11.2	10.6	10.9	10.7
	11.2	10.2	11.2	10.5	11.0	10.6	11.3	9.4	12.7	9.1
	11.5	10.5	11.0	10.6	11.0	10.6	10.9	10.7	10.8	10.6
	11.1	10.7	10.8	10.7	11.4	10.1	11.0	10.2	12.1	9.5
	11.6	10.2	11.6	9.9	11.4	9.8	12.1	10.1	10.8	10.8
	11.0	9.8	12.8	8.5	12.3	10.1	11.2	10.4	11.2	10.4
	11.1	10.5	11.1	10.5	11.0	10.7	10.8	10.8	11.0	10.1
040	11.8	9.9	11.1	10.7	10.9	10.6	11.5	9.9	11.7	9.5
	11.9	10.6	11.0	10.5	11.1	10.5	11.0	10.8	10.8	10.7
	11.0	10.5	11.0	10.6	11.1	10.2	11.4	10.4	10.9	10.8
	10.8	10.6	11.2	10.3	11.2	10.5	10.9	10.8	10.8	10.6

*1 ksi = 0.145 MPa

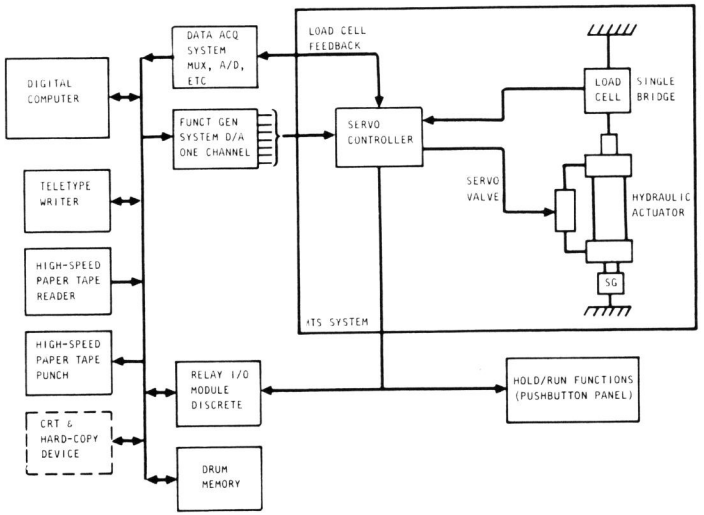

Fig. 4. Schematic of MTS and datum 70 systems.

CRACK GROWTH MODEL SELECTION

In the beginning of these research and development efforts, guidelines for selecting a load interaction model used in the projected crack-growth prediction methodology were established. The first criterion is that the load interaction model chosen should be capable of accounting for the effects of overload retardation, compressive load acceleration, and coupling effect, such as the reduction of overload retardation by compressive load cycles immediately following the overload cycles. The second criterion is that the model should be formulated based on the linear elastic fracture mechanics (LEFM) concept; i.e., fatigue crack-growth behavior is characterized by the variations of the stress-intensity-factor range, ΔK. The third criterion is that there should be no excessive data or lengthy computation needed in the application of such a model for production type of usage

Most of the existing load interaction models can be modified to fulfill the aforementioned criteria. It was decided to modify the generalized Willenborg model because of its wide usage in the aerospace industry in the United States. The generalized Willenborg model has been demonstrated to be adequate in predicting the tensile overload retardation effect for flight spectrum loadings (McGee, 1977). In mathematical form, the generalized Willenborg model can be expressed as:

$$(K_{max})_{eff} = K_{\infty_{max}} - \Phi \left[K^{OL}_{max} \left(1 - \Delta a/Z_{ol}\right)^{1/2} - K_{\infty_{max}} \right]$$

$$(K_{min})_{eff} = K_{\infty_{min}} \quad \Phi \left[K^{OL}_{max} \left(1 - \Delta a/Z_{ol}\right)^{1/2} - K_{\infty_{max}} \right]$$

$$\Phi = \left[1 - \left(K_{max_{th}}/K_{\infty_{max}}\right) \right] / \left(S_{so} - 1\right)$$

Where K_∞, K^{ol}, $K_{max_{th}}$ are the stress-intensity-factor values corresponding to the applied load, maximum overload, and threshold, respectively, Δa is the growth following overload, Z_{ol} is the overload retardation zone size, and S_{so} is the overload shutoff ratio.

The effective stress intensity factor range and stress ratio are thus equal to

$$(\Delta K)_{eff} = (K_{max})_{eff} - (K_{min})_{eff} = (\Delta K)_\infty$$

$$R_{eff} = (K_{min})_{eff}/(K_{max})_{eff}$$

Note that the effective stress-intensity-factor range $(\Delta K)_{eff}$ has the same value as the $(\Delta K)_\infty$; thus, the generalized Willenborg model accounts for the overload retardation effect by reducing the stress ratio below the remotely applied value.

The generalized Willenborg model does not account for the compressive load acceleration effect on the load cycle immediately following. It does not account for the reduction of the overload retardation effect when the overload is immediately followed by a compressive load either. Hence, overestimation on crack-growth lives will often result from the application of the generalized Willenborg model on spectrum loadings containing compressive load cycles, e.g., ground load cycles. Thus, improvement of the generalized Willenborg model to account for the compressive load effects is obviously needed.

IMPROVED CRACK-GROWTH METHODOLOGY

To properly account for the compressive load effects, the Chang acceleration scheme used in the Vroman/Chang model (Chang, 1979a) is adopted in the improved crack-growth methodology. The Chang acceleration equation takes the same form as the Walker equation (Walker, 1970); i.e., $da/dN = C\left[(1 - R)^q K_{max}\right]^n$, $R<o$. The exponent q in the equation is the acceleration index. When R is negative, the crack-growth rate accelerates by a factor of $(1-R)^{qn}$.

The reduction of the overload retardation caused by the compressive load immediately following the overload is taken care of by an effective overload interaction zone concept. The overload interaction zone size in the generalized Willenborg model is defined as:

$$Z_{ol} = \frac{\alpha}{2\pi}\left(\frac{K_{\infty}}{F_{ty}}\right)^2$$

Where $\alpha = 1$ for the plane stress condition and $\alpha = 1/2\sqrt{2}$ for plane strain condition. F_{ty} is the material yield strength.

The effective overload interaction zone size is assumed to be:

$$(Z_{ol})_{eff} = (1 + R_{eff})\ (Z_{ol}),\ R_{eff}<o$$

To avoid having the effective overload interaction zone size become negative, a cutoff valve of the effective stress ratio is set equal to -1.

Since the generalized Willenborg retardation model predicts the overload retardation by depressing the effective stress ratio below that remotely applied, the Walker rate equation, which accounts for the stress ratio effect, is chosen because the effective stress ratio is a positive condition. In conjunction with Chang's compressive load acceleration scheme, the proposed crack-growth methodology can be expressed as:

$$da/dN \begin{cases} = c\left[(1 - R_{eff})^{m-1}\ (\Delta K)_{eff}\right]^n, & R_{eff}>o \\ = c\left[(K_{max})_{eff}\right]^n, & \text{FOR } R_{eff} = o \\ = c\left[(1 - R_{eff})^{q}\ (K_{max})_{eff}\right]^n, & R_{eff}<o \end{cases}$$

where c, m, and n are crack-growth-rate constants determined from constant amplitude tests at various positive stress ratios and the acceleration index q is determined from negative stress-ratio tests.

TEST DATA CORRELATIONS

Crack-growth methodology discussed in the preceding is implemented into a computer program, EFFGRO, developed in-house at Rockwell (Szamossi, 1972). Baseline crack-growth-rate constants for 2219-T851 aluminum alloy and other parameters used in the correlation are shown in Fig. 5 and Table 2.

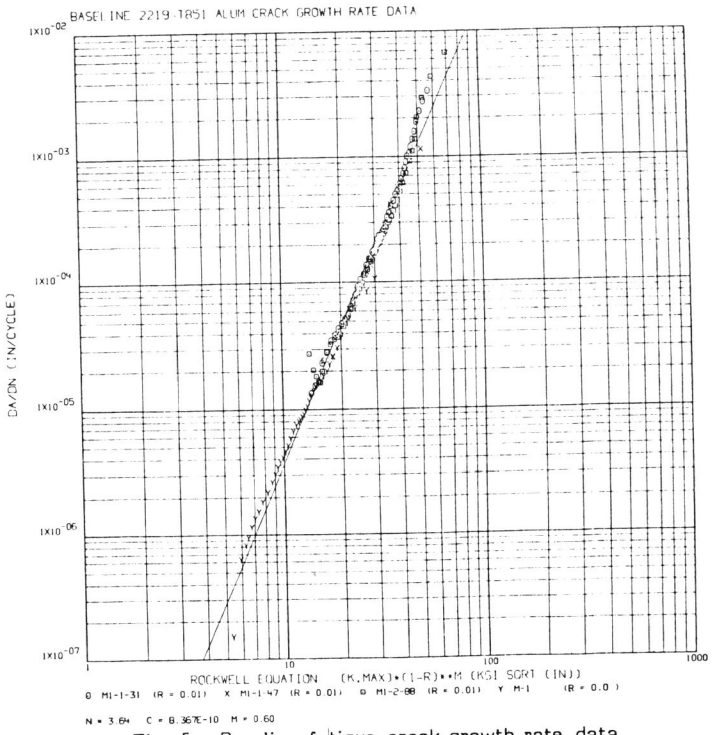

Fig. 5. Baseline fatigue crack-growth-rate data

Table 2 Crack Growth Rate Constants and Other Parameters Used in the Correlation Study

c	$= 8.367 \times 10^{-10}$	ΔK_{th}	$= 2.27\ (1 - R)$ MPa$\sqrt{m}$
n	$= 3.64$	R^+_{cut}	$= 0.75$
m	$= 0.6$	R^-_{cut}	$= -0.99$
q	$= 0.3$	S_{so}	$= 3.0$
α	$= 1$	k_c	$= 59.14$ MPa$\sqrt{m}$
F_{ty}	$= 5.15$ MPa		

All the input flight spectra were range-pair counted. Table 3 summarizes the crack-growth data correlation results. It showed that when using the proposed methodology, good correlation was achieved.

Table 3. Summary of Correlations on Fatigue Crack-Growth Data Generated under Random Spectrum Loadings

*R = N_{Pred}/N_{Test}

Test No.	Mission Type	σ_{lim} (σ_{max}) MPa	$c_{cm} - c_f$	Test Life Cycles	Analytical Predictions cyc.	R*
M-81	Fighter A-A	2.9	0.41-1.27	115,700	168,720	1.46
M-82	Fighter A-A	4.35	0.38-failure	58,585	53,312	0.91
M-83	Fighter A-A	5.8	0.38-failure	18,612	17,309	0.93
M-84	Fighter A-G	2.9	0.4-failure	268,908	368,662	1.37
M-85	Fighter A-G	4.35	0.37-failure	95,642	91,816	0.96
M-86	Fighter A-G	5.8	0.39-failure	36,367	29,093	0.8
M-88	Fighter I-N	4.35	0.38-failure	380,443	528,316	1.39
M-89	Fighter I-N	5.8	0.38-failure	164,738	184,507	1.12
M-90	Fighter mixed	2.9	0.38-failure	218,151	290,140	1.33
M-91	Fighter mixed	4.35	0.38-failure	65,627	65,630	1.01
M-92	Fighter mixed	5.8	0.38-failure	22,182	21,738	0.98
M-93	Transport	(2.03)	0.64-1.37	1,359,000	1,780,290	1.31
M-94	Transport	(2.84)	0.66-0.97	279,000	318,060	1.14

CONCLUSION

An improved methodology for predicting cyclic growth behaviors on cracks under random spectrum loading has been presented. Analytical predictions using a computer program which implements this methodology were correlated with experimental data. Results indicate that the proposed crack-growth methodology is adequate for use in the crack-growth analysis required in the fracture control plans on airframe structures.

ACKNOWLEDGEMENTS

This paper is based on part of the results of a study sponsored by the U.S. Air Force Wright Aeronautical Laboratories, Flight Dynamics Laboratory, Wright-Patterson Air Force Base, Ohio, U.S.A.

REFERENCES

Wheeler, O. E. (1972). Tran. of the ASME, J. of Basic Eng. 181-186.

Willenborg, J., Engle, R. M., and Wood, H. A. (1971). AFFDL-TR-71.

Gallagher, J. P (1974). AFFDL-TR-74-27.

Chang, J. B. (1979). AFFDL-TR-79-3036, Vol. I.

Elber, W. (1971). ASTM STP 486, 230-242.

Bell, P. D., and Wolfman, A. (1976). ASTM STP 595, 157-171.

Dill, H. D., and Saff, C. R. (1976). ASTM STP 595, 306-319.

Dill, H. D., and Young, M. T. (1977). AFFDL-TR-76-113.

McGee, W. M., and Hsu, T. M. (1977). AFFDL-TR-77-2, Vol. I.

Chang, J. B. (1979). Rockwell Report, NA-78-491-5.

Walker, K. (1970). ASTM STP 462.

Szamossi, M. (1972). Rockwell Report, NA-72-94.